Corrosion Behavior of Surface-treated Ferritic/Martensitic Steel in Liquid Sodium Environment

JeongHyeon Lee [a], Sang Hun Shin [b], Jung Ki Lee [a], Ji Hyun Kim [a*]
aUlsan National Institute of Science and Technology (UNIST), Ulsan, Republic of Korea
bKorea Atomic Energy Research Institute (KAERI), Daejeon, Republic of Korea
*Corresponding author: kimjh@unist.ac.kr

1. Introduction

Ferritic/martensitic steels are considered as candidates of cladding materials of Sodium-cooled Fast Reactors (SFRs).

Their compatibility with sodium is one of issues especially dissolution, chemical reaction, and carbon transfer with impurities, which degraded the mechanical properties. The compatibility of cladding and structural materials with sodium has to be carefully investigated, as sodium could promote corrosion of cladding and structural materials in two ways. One is produced by the dissolution of alloy constituents into the sodium, and the other is produced through a chemical reaction with impurities (especially oxygen and carbon) in the sodium environment [1].

Gr.92 is known as compatible in sodium environment because this steel possesses excellent properties [2]. For instance, Gr.92 has high creep and tensile strength, low thermal expansion coefficient. In the Ultra-long Cycle Fast Reactor (UCFR) which is developed in UNIST, however, cladding is exposed long-term in high temperature liquid sodium environment [3]. So, it is very important to investigate the corrosion-related behavior such as surface corrosion rate, carburization, decarburization and mechanical properties for its operation time.

The decarburization process where dissolved carbon near the specimen surface diffused in to the liquid sodium. This process can originate from the difference between dissolved carbon activity in the material and liquid sodium. A compatibility test the cladding tube revealed that a decrease of the mechanical property instigated by the aging proves governed the whole mechanical property [4].

SiC and Si$_3$N$_4$ Chemical Vapor Deposition (CVD) coating for decarburization barrier on the surface of FMS is considered in this study. The CVD coated specimens are experiment for compatibility of high temperature liquid sodium.

To monitor the corrosion behavior of these candidate materials in sodium environment, Electrochemical Impedance Spectroscopy (EIS) method was firstly introduced and investigated in this study. The use of the technique of impedance spectroscopy to measure the electrical impedance response of any oxide layers, SiC and Si$_3$N$_4$ that can be a one of solutions to this monitoring problem.

2. Experimental

2.1 Coating

Films of SiC and Si$_3$N$_4$ are typically grown on low-temperature substrates by plasma-enhanced chemical vapor deposition (PECVD). The integrated absorption intensity of the stretching mode of the Si-H and C-H bonds was calculated from the FT-IR spectra of the film. The capacitance and the geometric resistance (RΩ) of the ceramic associated with the liquid sodium environment can also be measured.

The material used was a normalized and tempered Gr.92 steel. The chemical composition of the test materials is shown in Table. 1. The samples were sanded to a finish of 400 grit, and were cleaned in ethanol, acetone, and distilled water.

The coating environment is 0.8Torr, 350°C and 1hour expose time for SiC coating, and 1.5Torr, 350°C and 1hour expose time for Si$_3$N$_4$ coating. The cross-sectional images of the SiC and Si$_3$N$_4$ coated Gr.92 are shown in Fig. 1. The thickness of the coating is 1 μm in each case.

2.2 Immersion Test

The immersion experiment was performed in the static autoclave in order to examine the effectiveness of the CVD coating as a function of the exposure time. Nine specimens were used in the immersion experiment: i.e., three specimens each of Gr.92, were coated with SiC and Si$_3$N$_4$, respectively. Dissolved oxygen is also saturated in the liquid sodium. Each specimens are taken out 100h, 200h and 300h, respectively. The EIS experiment was performed in glove box either. Three specimens were used in the EIS experiment: i.e., one specimens each of Gr.92, were coated with SiC or Si$_3$N$_4$, respectively. Impedance is measured during exposure time.
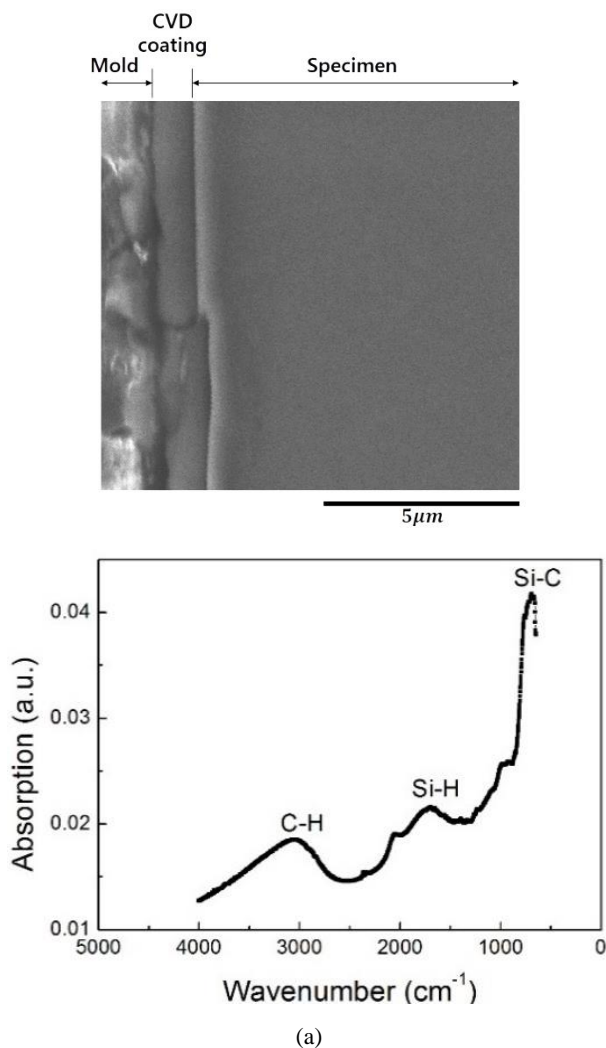
The FT-IR data of the PECVD-coated specimens is shown in Fig. 1. In Fig. 1 (a) and (b), the stretching mode of the Si-C, Si-H, and C-H bonds is revealed by a strong peak at 790 cm^{-1} and weak ones near 1800-2000 and 3000cm^{-1}, respectively; the weak peak near 1250cm^{-1} correspond to the bending mode of Si-CH$_3$. Similarly, the strong peak at 900-1000cm^{-1} (Fig. 1 (b)) corresponds to the stretching mode of the Si-N bond. These data verify that the CVD coating is well-

deposited on the surface of the specimens; i.e., respective peaks at 790cm^{-1} (Fig. 1 (a)) and 900-1000cm^{-1} (Fig.1 (b)) confirm the presence of SiC and Si$_3$N$_4$ [5].

Liquid sodium is located at the stainless steel autoclave in the glove box and dissolved oxygen is saturated in the liquid sodium to accelerate the corrosion by making the environment more corrosive.

Table I: Chemical composition of the test material (wt%)

	C	Si	Mn	Cr	Ni	Mo	W	V
Gr.92	0.087	0.21	0.41	8.69	0.13	0.38	1.62	0.18

(a)

2.3 EIS measurement

Impedance measurements were m zade using a 273A potentiostat (Princeton Applied Research, US) and SI 1260 impedance analyzer (Solartron Analytical, US). These measurements were performed at 550 °C-650°C and an AC amplitude the Z view® impedance analysis software to extract the electrical properties of the oxide.

Experiment was performed on reactor installed at glove box. The electrical path from the liquid sodium to EIS measurement system should be insulated from the glove box.

Insulation constitutes an important part of the electrical experiment. Therefore, care was taken to prevent electrical short-circuits and each electrode and thermocouple functioned as an insulating ceramic device in this regard.
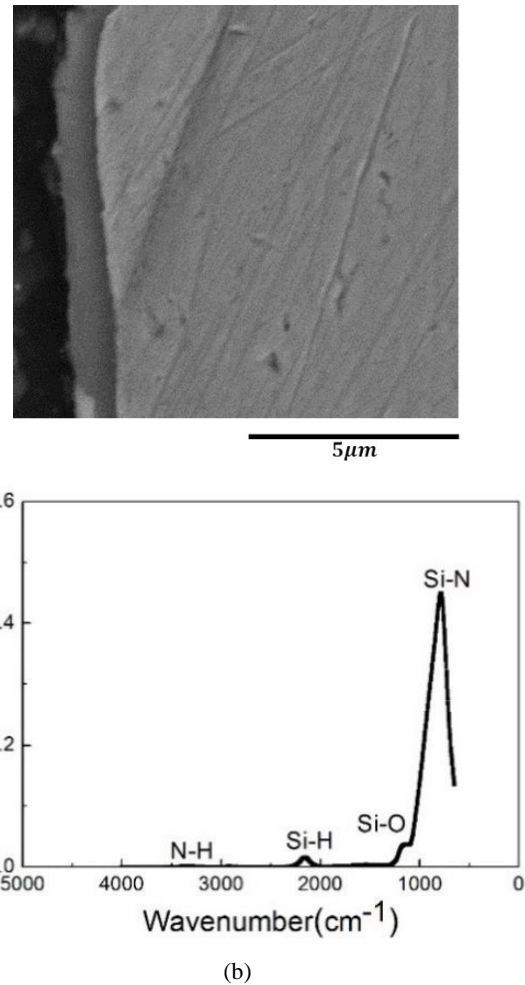

(b)

Fig. 1. SEM image of the cross section and FT-IR results of (a) SiC- and (b) Si3N4-coated Gr.92.

3. Results

3.1 Corrosion experiment of CVD coated FMS

The corrosion experiment to determine the effectiveness of the CVD coatings was performed by exposing the samples for a total of 300h to the 550°C liquid sodium environment. Plotting the corresponding weight change as a function of the exposure time (Fig. 2) reveals that the coated specimens experience greater weight loss than their uncoated counterparts; this greater

loss results from loss of the coating from the surface of the specimens. From the SEM and the weight change analysis, the SiC-coated and Gr.92 specimens experience less weight loss than their Si_3N_4 counterparts. It can be verified the SiC materials is more stable than Si_3N_4 materials.

In the result of 100h of Fig. 2, weight loss is observed in all specimen. The flux of metal dissolution is bigger than oxidation. Both SiC and Si_3N_4 are lost coating in liquid sodium. It can be checked at Fig. 3 (a) and Fig. 3 (b). Especially, all Si_3N_4 coating was lost from specimen. According to this reason, weight loss of Si_3N_4 is biggest in Fig. 2. The Si_3N_4 specimens change the corrosion rate at exposed area by peeling off coating. Also, SiC specimen has part of peel off coating. From this result, it show the SiC coating remains relatively more than Si_3N_4. The weight loss results look like SiC and Si3N4 coated specimen results is higher than as-received specimen results. However, the results of weight loss include the coating weight.
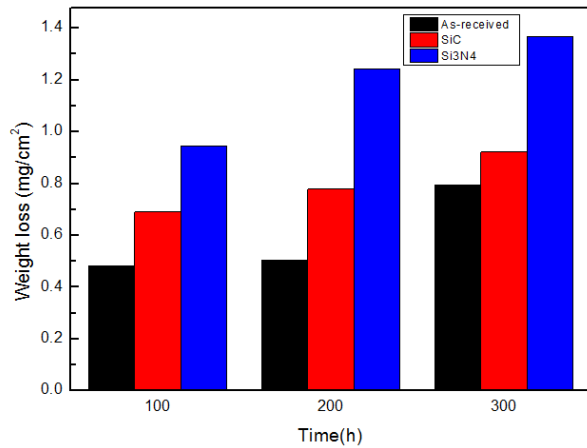

Fig. 2. Dependence of weight loss on the exposure time of Gr.92 in 650ºC sodium.

In order to explain the existence of $NaCrO_2$, EDS analysis is performed to mapping analysis and point analysis. In the EDS analysis, it is observed the $NaCrO_2$ formed on the surface of specimen by detecting the peaks of O, Na and Cr in the same position. The oxidation behavior is observed at the surface which the coating has removed from specimen. Also, a1, b1, c1 show the SiC particle and a2, b2, c2 show the NaCrO2 from energy dispersive X-ray spectroscopy (EDS) measurements in the Fig. 4 (a).

Figure 4 shows the cross-sectional SEM images of As-received, SiC coated and Si_3N_4 coated specimens, which were immersed 650°C sodium for 300h on which ~8.53μm, ~2.33μm and 3.19μm thick Cr-rich zone were formed, respectively. The depths of coated specimens are smaller than one of as-received specimen. The one of SiC coated specimen is the smallest because the exposure time without coating is relatively short. The cross section analysis is performed for the detail analysis.

The results of line profiling reveals that there is Cr-rich zone look like dark site near the surface of specimen in Fig. 4 (b). In the point 1, besides, the result of EDS shows the Cr-rich zone. Besides, O and Na peak are observed in the dark area in Fig. 4 (c). In the point 2, the result shows the similar result with point 3 which is basic material from EDS analysis. From these results, it can be verified the Na and O were role of driving force of Cr-rich zone.
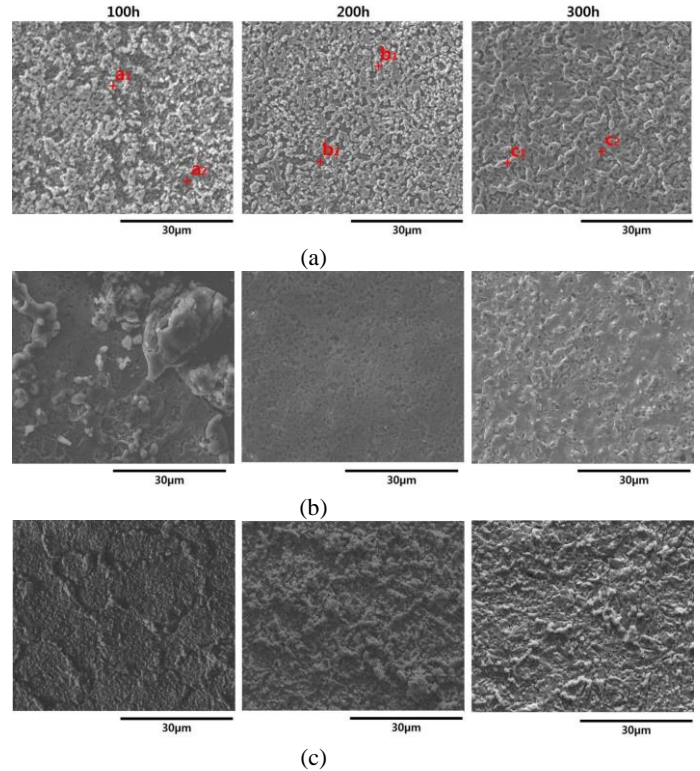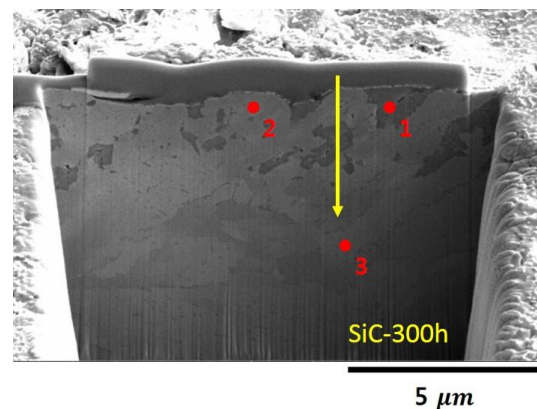

Fig. 3. Surface of (a) As-received Gr.92 specimens (b) Si3N4 coated Gr.92 specimens. (c) un-coated Gr.92 specimens for as-received specimen exposure to 650°C sodium
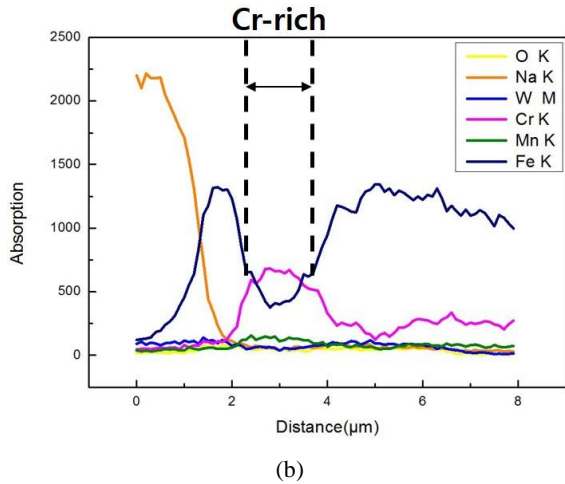

(a)

(b)

Fig. 4. FIB-EDS analysis results of SiC coated specimen in 650°C sodium (a) SEM image (b) line profiling

3.2 Electrochemical experiment

EIS has also been used to investigate oxidation kinetic of metals in Lead-Bismuth Eutectic (LBE)-cooled systems that simulate reactor environments [6]. The equivalent circuit (EC) used to model the data is similar to the simplified Randles equivalent circuit. The Randles equivalent circuit is used for the corrosion of metals without the formation of protective oxide. Therefore, it can be applied to Randle's Circuit. The $NaCrO_2$ is formed the island oxidation. It is different the passive Randle's Circuit. The Randle's circuit represents the polarization resistance, however the in this experiment.

Electrochemical impedance spectra for the passive films on the FM steel were measured over a wide range of frequencies in 650°C liquid sodium. EIS data imply that the thickness and current are depended on time. The impedance increased steadily over the entire 300h exposure period of the experiment. Figure 6 shows the resulting Nyquist plot of the specimen at four different times during the corrosion experiments in 650°C sodium. The EIS results verify the formation of oxides and the tendency for oxide growth in the specimen surface.

In accordance with the result of As-received specimen, the EIS results verify the formation of oxides, resistance of oxide and the tendency for oxide growth in the specimen surface in Fig. 5.

Figure 6 shows the Nyquist plot of SiC coating on Gr.92 in liquid sodium When SiC coating is exposed to sodium for 200h, size of semicircle become smaller than before in Nyquist plot in Fig. 6 (a). The result of 200h and 300h show similar behavior with early stage of Gr.92 corrosion in sodium in Fig. 5. From the EIS result, SiC coating is adhered to specimen surface well until 100h.

Figure 7 shows the Nyquist plot of Si_3N_4 coating on Gr.92 in liquid sodium When Si_3N_4 coating is exposed to sodium for 100h, size of semicircle become smaller than before in Nyquist plot in Fig. 7 (a). The results of 100h, 200h and 300h show similar behavior of Gr.92 corrosion in sodium described in Fig. 5. From the EIS result, Si_3N_4 coating is adhered to specimen surface well between 0h and 100h.

The resistance of oxides grows up depend on exposure time. In the Fig. 8, it can be checked the coating existence by resistance. Based on the EIS results, it is expected that SiC coating disappeared on the surface between 100h and 200h of the exposure times, and Si_3N_4 coating disappeared on the surface between 0h and 100h of the exposure times. Both coatings were maintained during too short term. Also, it is observed that the SiC coating is more stable than Si_3N_4 in high temperature liquid sodium.

From the resistance of EIS experiment, the coating existence can be checked by resistance. The SiC coating was maintained during the relatively long time. In that, the exposure time without the coating or the barrier on corrosion is different each other. The result of corrosion level of As-received specimen is more than Si_3N_4 coated specimen, and Si_3N_4 coated specimen is more than SiC coated specimen from resistance change from Fig.8.
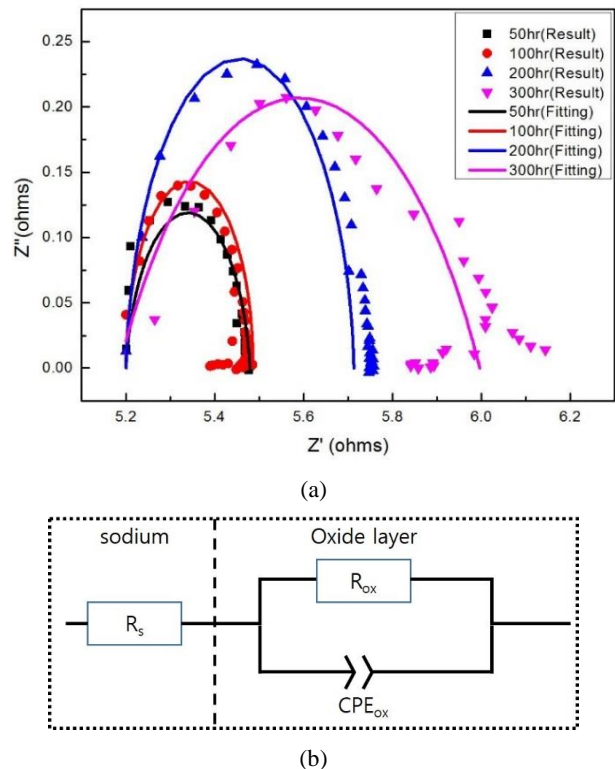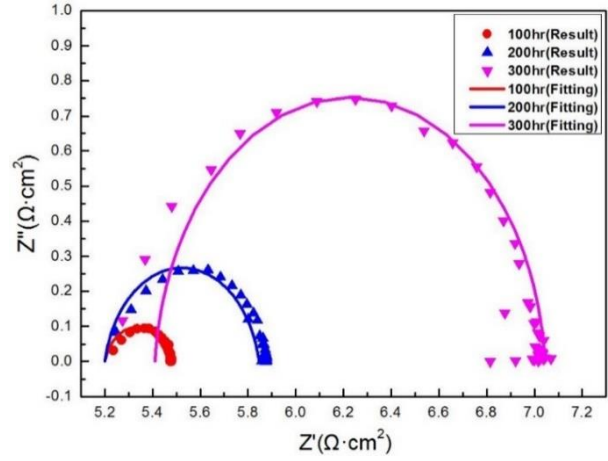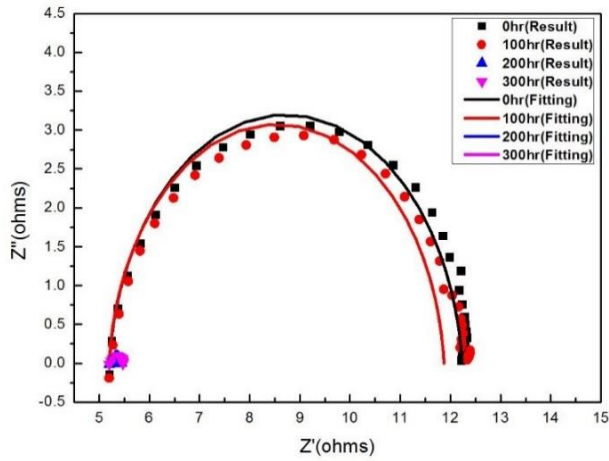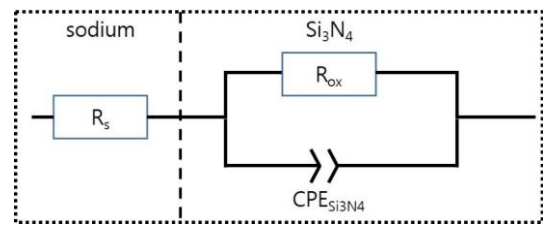

(a)

(b)

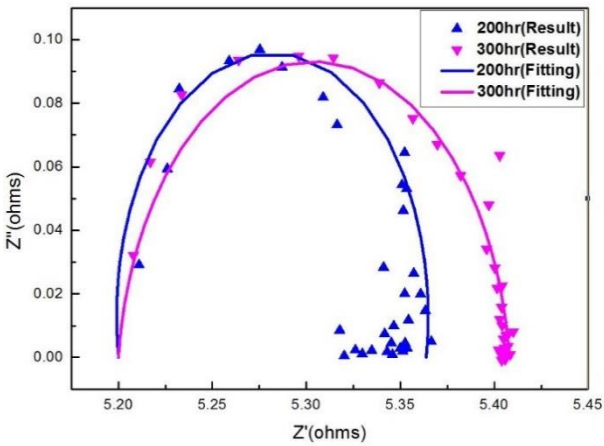Fig. 5. (a) Nyquist plot of Gr.92 specimen in liquid sodium at 650°C (b) equivalent circuit
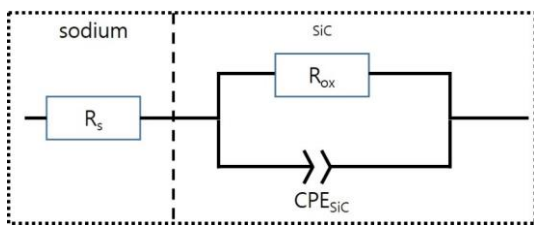
(a)

(b)

Fig. 6. (a) Nyquist plot of SiC coating on Gr.92 specimen in liquid sodium at 650°C and enlarged graph (b) equivalent circuit.
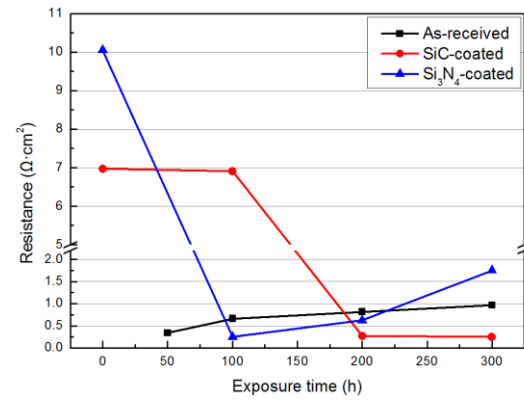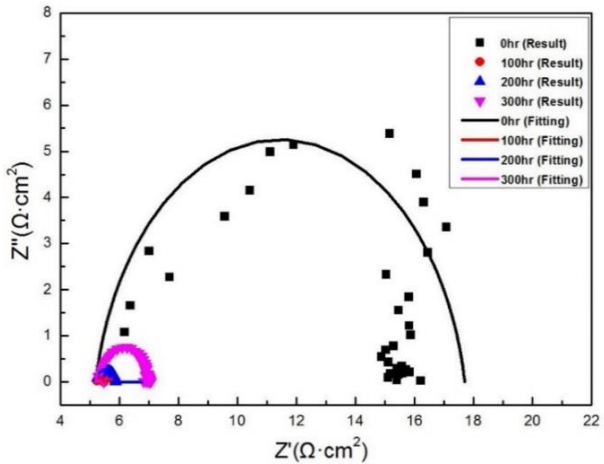

(a)

(b)

Fig. 7. (a) Nyquist plot of Si3N4 coating on Gr.92 specimen in liquid sodium at 650°C and enlarged graph (b) equivalent circuit.

Fig. 8. Resistance of exposed specimen depend on exposure time in 650°C sodium.

4. Conclusions

In this study, as-received and surface-treated Gr.92 specimen in the oxygen-saturated liquid sodium were examined at high temperature for 300h. The impedance results reveal the information for the corrosion behavior in liquid sodium. Also, microstructure results reveal the information for the maintenance of coating and role of coating. Main results are as follows:

i. From the EIS analysis, the SiC coating is more stable than Si_3N_4 in high temperature liquid sodium. And EIS results verify the formation of

oxides and the tendency for oxide growth in the specimen surface.

ii. From the microstructure analysis, the results reveal that there is Cr-Na-O rich zone under the surface. And, coated specimen shows that depth of the affected region is shorter than as-received. Also, it is observed that the SiC coating is little more stable than Si_3N_4 in high temperature liquid sodium.

iii. With the EIS method, it can be verified the existence of coating on the specimen. And, the microstructure analysis is well shown similar data which is the EIS data in coating existence

The coating on the cladding can be a protective film. In order to make more protective film for corrosion and dissolution, however, it has to solve the keeping of coating on the steel surface.

ACKNOWLEDGEMENTS

REFERENCES

[1]   T. Furukawa, S. Kato, E. Yoshida, J. Nucl. Mater. 392 (2009) 249.

[2]   S. Alsagabi, T. Shrestha, I. Charit, J. Nucl. Mater. 453 (2014) 151.

[3]   J.A. Jung, S.H. Kim, S.H. Shin, I.C. Bang, J.H. Kim, J. Nucl. Mater. 440 (2013) 596.

[4]   J.H. Kim, S.H. Kim, J. Nucl. Mater. 443 (2013) 112.

[5]   B. Balland, R. Botton, M. Lemiti, J.C. Bureau, a Glachant, 24 (1993) 389.

[6]   R.S. Lillard, M. Paciotti, V. Tcharnotskaia, J. Nucl. Mater. 335 (2004) 487.